Actuator Fault-Tolerant Control for an Electro-Hydraulic Actuator Using Time Delay Estimation and Feedback Linearization

VAN DU PHAN[ID]**, CONG PHAT VO**[ID]**, HOANG VU DAO**[ID]**, AND KYOUNG KWAN AHN**[ID]**, (Senior Member, IEEE)**

School of Mechanical and Automotive Engineering, University of Ulsan, Ulsan 44610, South Korea

Corresponding author: Kyoung Kwan Ahn (kkahn@ulsan.ac.kr)

ABSTRACT This article proposes a novel fault-tolerant controller for a double-rod electro-hydraulic actuator whilst the motion control system faces with system disturbances/uncertainties and internal leakage fault. Firstly, taking the advantage of the coordinate transformation, the nonlinear system is converted to a linear system to apply the control design tools in linear control theory. Besides, the matched, mismatched disturbances, and internal leakage fault are integrated into a new lumped uncertainty based on this transformation. Inspired by the great capability of time delay estimation technique, the suggested controller is developed to effectively detect and compensate for the internal leakage fault. To enhance the performance of the control system, an adaptive integral sliding mode control approach is deployed to effectively suppress the lump estimated error, and the effects of fault. The perfect combination of input-output feedback linearization, adaptive integral sliding mode, and time delay estimation is investigated to achieve high-precision tracking control and strong robustness in the presence of matched, mismatched disturbances, and faults, simultaneously. Moreover, the global stability of the suggested control algorithm is demonstrated by the Lyapunov theory. Finally, several tracking performance comparisons of the proposed approach with the existing controllers to demonstrate the efficiency are exhibited through simulation analyses and experiment results.

INDEX TERMS Time delay estimation, feedback linearization, fault detection, fault-tolerant control.

I. INTRODUCTION

Recently, electro-hydraulic actuators (EHAs) have been accustomed increasingly popular in industrial applications such as aircraft actuators, blade pitch actuators for the wind turbine, robotics, and vehicle suspension due to their ability to generate large force output, fast response, and so on. Nonetheless, the presence of high nonlinearity features, disturbances, uncertainties as well as faults prevents the improvement of tracking control performance for EHAs [1]–[3]. So, the investigation of the advanced control algorithm to tackle the aforementioned issues has been paid a lot of attention [4]–[10].

In order to deal with the impact of disturbance/uncertainty, several effective methods have been investigated. First,

The associate editor coordinating the review of this manuscript and approving it for publication was Dazhong Ma[ID].

the disturbance observer methods (e.g., nonlinear disturbance observer (DO) [5], [6], extended state observer (ESO) [7]–[10]) and approximation techniques (e.g., fuzzy neural network [11], [12], time delay estimation (TDE) [13]) are integrated into control scheme, whilst the disturbance/uncertainty is compensated to enrich the control performance. Besides, the instability can be avoided due to the selection of lower gains of the controller. Second, an adaptive gain control law is presented that adopts the parametric uncertainties [14], [15]. However, the influence of external disturbance cannot completely remove. The other notable methods are introduced in the previous research such as an online parameter adaptation mechanism [16], a state estimator-based minimal learning parameter (SE-MLP) [17], robust output feedback control [18] etc. In reality, the disturbances/uncertainties may become faults that seriously deteriorate the control performance or even

become unstable [19], [20]. Considering the EHA system, it is well known that faults happen relating to the sensor components, hydraulic cylinder, power supply, and so on [2]. Especially, the internal leakage fault considering as actuator fault often occurs that affects the control performance, reliability as well as safety problems. In [21] and [22], a leakage fault estimation algorithm is designed by using ESO/DO under lumped disturbances for the EHA but the main disadvantage of this approach is the necessary of two observers and a complex identification algorithm for the internal leakage fault. Additionally, the feasibility in practice has not been resolved yet. In [23], a nonlinear representation learning approach was employed to detect leakage fault. However, the drawbacks of the uses of learning methods are the complexity in the training of neural networks as well as a burden computation. Meanwhile, owing to model-free, fast response, less complex, and robust properties, the TDE technique is an efficient solution to handle the system disturbances/uncertainties [24], [25]. Moreover, the application of TDE to detect and estimate fault for the EHA system has still been an open problem. Therefore, taking the advantage of TDE to elaborate the effective fault detection (FDTDE) is necessary to limit the hazardous malfunction in tracking control problem.

Since a fault is detected, the construction of the fault-tolerant control (FTC) scheme should be conducted to alleviate the influence of faults. To develop the FTC scheme, various types of control methods are presented such as integral sliding mode control (ISMC) [26], adaptive control [27], intelligent control [28], and so on. Among them, the ISMC has received considerable attention for many practical applications because of the impressive benefits for instance high robustness, reduced steady-state error, pursuing finite-time stability [29]–[31]. Besides, several important research results including [32]–[35] have introduced the outstanding properties of feedback linearization (FBL). This technique effectively cancels the nonlinearity characteristic of a nonlinear system and puts mismatched disturbances in a similar channel with new virtual input. Nevertheless, the analysis of FTC-based FBL has still been considered. Furthermore, the hybrid control methods which incorporate the TDE with FBL, ISMC, have not been investigated to handle the effect of the lumped disturbances as well as deal with the failure problems in the previous works.

Motivated by the above analysis, in this article, we present a TDE combined FBL, adaptive ISMC (AISMC) to cope with the actuator fault-tolerant tracking control problem of the EHA. Firstly, a coordinate transformation is used to convert the original system becoming a linear system to reject the inherent nonlinear features. Besides, the new lumped uncertainty is formulated including matched, mismatched disturbance, and the fault. Next, the FDTDE technique is deployed to approximate the given lumped uncertainty. The fault is successfully detected and accommodated when the estimated new lumped uncertainty is larger than a predefined threshold. Then, the estimated value via the TDE, and an adaptive law

are integrated into the ISMC which increases the robustness property to against the lumped disturbances, and faults. The proposed FTC exhibits high precision tracking control as well as system stability under both healthy and faulty conditions. The main contributions of this article can be provided as follows:

1) To the best of the author's knowledge, the FDTDE term is firstly proposed for the practical EHA.

2) The proposed FTC scheme is designed by the incorporation of the FDTDE, AISMC, and FBL controller to not only obtain strong robustness but also ensure both performance and safety under uncertainties/disturbances as well as faults.

3) The effectiveness of the proposed control approach is demonstrated in comparisons of both theoretical and experimental aspects in presence of the matched, mismatched disturbances, and internal leakage fault simultaneously.

This research paper is organized as the following: In section II, the system description of the EHA is presented. Section III shows the fault detection (FD) method and develops a novel active FTC. Sections IV and V discuss the simulation analyses and experiment results, respectively. Finally, the conclusions are summarized in Section VI.

II. SYSTEM DESCRIPTIONS
A. NONLINEAR EHA MODEL WITH FAULT AND PROBLEM FORMULATION
The simplified schematic diagram of the EHA is described in Fig. 1. The system consists of a hydraulic pump, a servo valve, a double-rod cylinder, and measurement components, i.e., a displacement transducer and two pressure sensors.
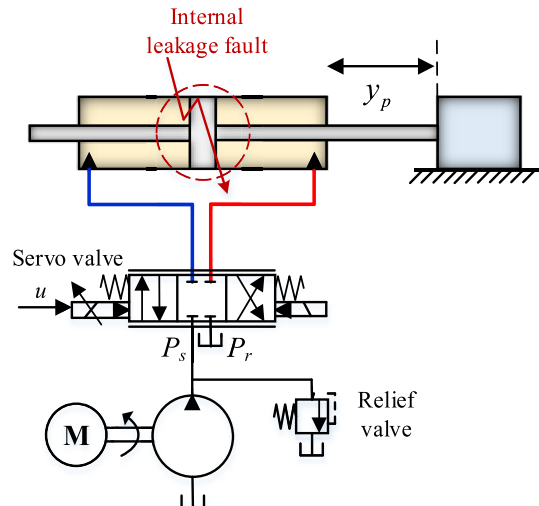
FIGURE 1. Schematic model of a double-rod EHA.

By applying the continuity equation, the flow rate dynamics through the cylinder is expressed by [1], [36]

$$Q_L = A\dot{y} + \frac{V_c}{4\beta_e}\dot{P}_L + q_L - Q_{Li} \qquad (1)$$

where A, V_c, and q_L are a ram area, a fixed control volume of the cylinder, and the internal leakage, respectively. β_e is the Bulk modulus. Q_{Li} is the time-varying deviation model including unmodeled pressure dynamics, modeling error, etc.

Assumed that the control supplied to the servo valve is directly proportional to the spool displacement. Hence, Q_L is load flow rate which is described with respect to control signal by

$$Q_L = k_t u \sqrt{P_s - sign(u) P_L} \quad (2)$$

where P_s is the supply pressure, k_t is a proportional gain of the servo-valve, $P_L = P_1 - P_2$ denotes the difference of pressure, P_i is the pressure value of ith chamber ($i = 1, 2$), u is the control signal supplied by the controller, and $sign(\bullet)$ is the standard signum function.

The reason for selecting the internal leakage fault is explained by its serious failures as well as the frequent occurrence in the practical EHA system. Since the internal leakage fault happens, it can be represented as [37], [21]

$$q_L = C_0 P_L + C_t \sqrt{|P_L|} sign(P_L) \quad (3)$$

where C_0 is the nominal coefficient of the internal leakage of the double cylinder; C_t is the internal leakage fault coefficient. It is noteworthy that the leakage fault coefficient C_t has a value range analysis from the slight to the abrupt fault. In this article, to reflect the effect of fault, the slow-varying faulty coefficient is indicated as the following.

$$C_t = \begin{cases} 0 & \text{if } t < T_m \\ (1 - e^{-\alpha(t - T_m)}) C_{t0} & \text{otherwise} \end{cases} \quad (4)$$

where T_m is the time of appearance of the fault, $\alpha > 0$ describes the evolution rate of the unknown fault. For the small value of α, the fault feature is increasing slowly, namely, an incipient fault. Otherwise, the leakage fault coefficient C_t approaches a step function in case of a large value of α and is called an abrupt fault.

Let us consider the mechanical dynamics given by Newton's second law as follows:

$$m\ddot{y} = P_L A - B\dot{y} + \Lambda(t, y, \dot{y}) \quad (5)$$

where y, m, and B represent the displacement, mass of the load, and viscous damping coefficient, respectively; $\Lambda(\bullet)$ is a lumped disturbance/uncertainty term including external load, nonlinear friction.

Choosing $x = [x_1, x_2, x_3]^T [y, \dot{y}, P_L]^T$ as the state variables. From (1)–(5), the EHA system can be described by the following third-order nonlinear state-space model:

$$\begin{cases} \dot{x}_1 = x_2 \\ \dot{x}_2 = g_a x_3 - g_b x_2 + d_1(x_1, x_2, t) \\ \dot{x}_3 = -h_b x_3 - h_c x_2 + h_a \\ \sqrt{P_s - x_3 sign(u)} u + \Delta(x_1, x_2, x_3, t) \end{cases} \quad (6)$$

where

$$g_a = \frac{A}{m}, g_b = \frac{B}{m}, d_1(x_1, x_2, t) = \frac{\Lambda(x_1, x_2, t)}{m},$$

$$h_a = \frac{4\beta_e k_t}{V_c}, h_b = \frac{4\beta_e C_0}{V_c}, h_c = \frac{4\beta_e A}{V_c}.$$

$\Delta(x_1, x_2, x_3, t) = d_2(x_1, x_2, x_3, t) + f_a(x_3, t)$ denotes the lumped uncertainty term that consists of the matched disturbances term d_2 and internal leakage fault, which are considered by the equations below

$$\begin{aligned} d_2(x_1, x_2, x_3, t) &= h_d Q_{Li}, \\ f_a(x_3, t) &= -h_d C_t \sqrt{|x_3|} sign(x_3) \end{aligned} \quad (7)$$

where $h_d = \frac{4\beta_e}{V_c} = \frac{h_a}{k_t}$

Assumption 1:

a) The reference signal $y_d = x_{1d}(t)$, its velocity, and acceleration are bounded.

b) The condition P_1, P_2, and $|P_L|$ sufficiently smaller than P_s is satisfied under a normal working condition in a real EHA system.

c) The d_1, $\dot{d}_1$, d_2, f_a, exist and are bounded, i.e., $|d_1| \leq D_1$, $|\dot{d}_1| \leq D_2$, $|d_2| \leq \delta_1$, $|f_a| \leq \delta_2$ where D_1, D_2, δ_1, δ_2 are positive constant.

B. MATCHED, MISMATCHED DISTURBANCE, AND INTERNAL LEAKAGE FAULT

In the EHA system, there are mismatched and matched disturbances as well as faults from several sources that influence the tracking performance of the closed-loop system. The matched and mismatched disturbance can be distinguished via its appearance with respect to the control input u. If one above listed component is in a similar channel with u, it is considered as matched disturbance, and vice versa [4], [38], [39].

In (6), the component of d_2 is the matched disturbance that arises from leakages in the hydraulic dynamics, non-linear uncertainties (i.e., parametric uncertainty and model uncertainty). Meanwhile, for mismatched disturbance, these components including viscous friction, Coulomb friction, unknown external load are lumped in d_1. In the real EHA system, the exact mathematical model of the mismatched disturbances is not easy to obtain. So, for the sake of convenience, without loss of generality, it is hypothetical and can be denoted according to the following expression [34], [40]:

$$d_1 = \frac{\Lambda}{m} = -k_f x_2 - f_c sign(x_2) - F_{ext}; \quad (8)$$

where k_f, f_c, and F_{ext} represent the ratio of viscous, Coulomb friction coefficient, and external load to mass, respectively.

The fault occurs in a practical system that can be categorized as three main groups: sensor fault, actuator fault, and component fault [19]. In the hydraulic system, the internal leakage fault is a relatively common malfunction that not only decreases the performance of the system but also causes serious damage. This fault often comes from a piston seal or internal flow loss [41]. The mathematical model of the internal leakage fault is described in (7). So, to overcome the effect of the above problem, it is necessary to design the advantage control that can guarantee good tracking control as well as retain the stability system.

Remark 1: The parameters g_a, g_b, h_a, h_b, and h_c are determined through the identification process, k_t is computed from the servo valve's datasheet. Then, the physical parameters of the EHA system such as A, B, m, β_e, C_0, and V_c can be carried out. The reader-interest can find the details of several identification algorithms for the system parameters in [42]–[44].

Remark 2: Because of the impossible of derivative of sign function, without loss of generality, the discontinuous term *sign* is replaced by a hyperbolic tangent function, namely, *tanh*. Besides, this hypothesis is to make the non-differentiable *sign* becoming continuously differentiable through *tanh* function and to support the control system design process [32], [34].

Remark 3: The control objective is to design a controller u that drives the output y of the EHA to track the reference trajectory y_d, despite the external disturbance, model uncertainty, and actuator fault. Motivated by the FDTDE and FBL, the novel FTC is developed such that the control objective for the nonlinear system (6) has been obtained.
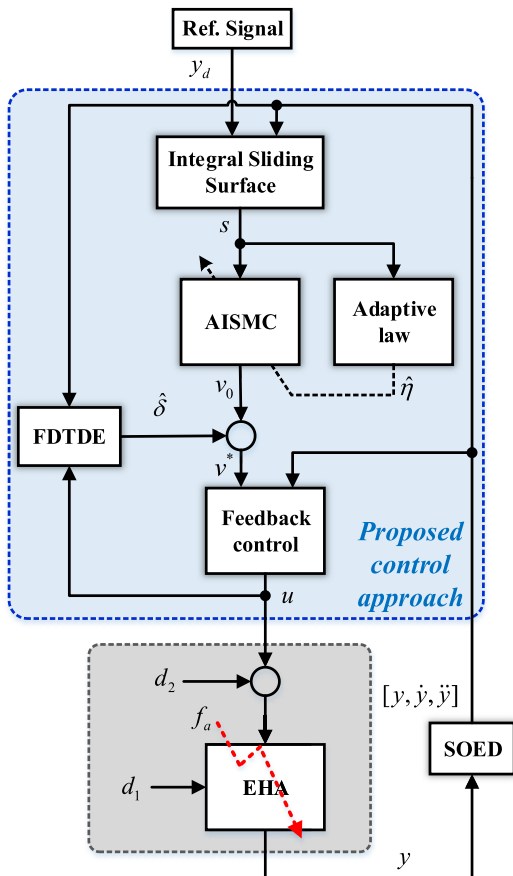

FIGURE 2. Structure of the proposed control scheme.

III. PROPOSED CONTROL DESIGN FOR EHA

The overall structure of the proposed FTC is shown in Fig. 2, which comprises three main steps. Firstly, the coordinate transformation using the Lie derivative is investigated in

which the disturbance, uncertainty as well as fault are considered. Inspired by this transformation, the nonlinear characteristic of the system is eliminated. It is primary to apply the control design tools in linear control theory for the nonlinear object. Then, the TDE technique is developed to not only estimate matched and mismatched disturbance but also detect the fault. Finally, the tracking control law is achieved by the combination of a pole placement technique, adaptive integral sliding mode, and FDTDE. Although the simultaneously concerned faults, matched and mismatched disturbance emerge in the EHA system, the proposed control scheme provides the system stability as well as a low steady-state error, and high precise control.

A. COORDINATE TRANSFORMATION AND SYSTEM MODEL TRANSFORMATION

As above-mentioned, based on the differential geometry theory, a design procedure of coordinate transform is derived. For further convenience in designing the FBL, the nonlinear system (6) is rewritten as follows:

$$\dot{x} = \phi(x) + \varphi(x)u + d(x, t)$$
$$y = \xi(x) \quad (9)$$

where $x \in R^m$, $u \in R^m$, $y \in R^m$ are state, control, and output vectors, respectively. $\phi = [x_2, g_a x_3 - g_b x_2, -h_b x_3 - h_c x_2]^T$, $\varphi = [0, 0, h_a \sqrt{P_s - x_3 sign(u)}]^T$, and $\xi(x)$ are smooth functions. The lump disturbance is given by $d = [0, d_1, \Delta]^T$. The Lie derivatives of the output ξ along the vector field $\phi(x)$ is denoted $L_\phi \xi(x)$. It can be calculated by using symbolic computation software or manual computation, and expressed by

$$L_\phi \xi(x) = \frac{\partial \xi(x)}{\partial x} \phi(x) \quad (10)$$

This notation can be used iteratively, that is

$$L_\phi^k \xi(x) = L_\phi L_\phi^{k-1} \xi(x) = \frac{\partial L_\phi^{k-1} \xi(x)}{\partial x} \phi(x) \quad (11)$$

where $k \geq 0$ is an integer with $L_\phi^0 \xi(x) = \xi(x)$

Definition 1: The system (9) has a relative degree ρ if the following conditions are satisfied [45]:

$$L_\varphi L_\phi^k \xi(x) = 0, \text{ for } k = 0, \ldots, \rho - 2$$
$$L_\varphi L_\phi^{\rho-1} \xi(x) \neq 0 \quad (12)$$

With the definition of relative degree ρ, the system can be considered as full state feedback linearizable, if the system has a well-defined relative degree ρ which equals the system order. The change of coordinate is described by

$$\psi_i = \xi^{(i-1)}, i = \overline{1, \rho} \quad (13)$$

Then, the exact input-output FBL is obtained, and the ρth derivation of output y can be expressed as [45]:

$$y^{(\rho)} = v = L_\phi^\rho \xi + L_\varphi L_\phi^{\rho-1} \xi u \quad (14)$$

By applying the FBL technique for the EHA system, the relative degree is firstly determined, $\rho = 3$ according to Appendix A. Then, the original nonlinear system (9) taking into account the perturbation model can be changed into an integral chain pseudo linear system model with composite disturbance as follows:

$$\psi = \begin{bmatrix} \psi_1 \\ \psi_2 \\ \psi_3 \end{bmatrix} = \begin{bmatrix} y \\ \dot{y} \\ \ddot{y} \end{bmatrix} = \begin{bmatrix} \xi \\ L_\phi \xi + L_d \xi \\ L_\phi^2 \xi + L_d L_\phi \xi + \frac{d}{dt}(L_d \xi) \end{bmatrix} \quad (15)$$

Then, the derivative of (15) is described by

$$\dot{\psi} = \begin{bmatrix} \dot{\psi}_1 \\ \dot{\psi}_2 \\ \dot{\psi}_3 \end{bmatrix} = \begin{bmatrix} \dot{y} \\ \ddot{y} \\ \dddot{y} \end{bmatrix} = \begin{bmatrix} \dot{y} \\ \ddot{y} \\ v + \delta \end{bmatrix} \quad (16)$$

where $v = L_\phi^3 \xi + L_\varphi L_\phi^2 \xi u$, $\delta = L_d L_\phi^2 \xi + \frac{d}{dt}(L_d L_\phi \xi) + \frac{d^2}{dt^2}(L_d \xi)$. Herein, v and δ denote a new input variable and a new lumped disturbance, respectively.

To simplify the notations, (16) can be rewritten by

$$\dot{\psi} = A\psi + Bv + \Omega \quad (17)$$

where $A = \begin{bmatrix} 0 & 1 & 0 \\ 0 & 0 & 1 \\ 0 & 0 & 0 \end{bmatrix}$, $B = \begin{bmatrix} 0 \\ 0 \\ 1 \end{bmatrix}$, $\Omega = \begin{bmatrix} 0 \\ 0 \\ \delta \end{bmatrix}$.

Remark 4: The coordinate transformation converts the original system (6) to the equivalent linear system (17) in which the mismatched disturbance, matched disturbance (i.e., external load, parametric uncertainty), and fault are integrated into the new lumped disturbance. The benefit of this technique makes the initial complex system becoming simple and easy to implement control design procedures.

Remark 5: It is noted that the variable ψ is derived from the output signal y. Herein, the only available position sensor based on the displacement transducer information, $y = x_1$ can be measured. Nevertheless, in the control design procedure, other states such as the velocity and acceleration need to know. To obtain the information of the velocity and acceleration, a second-order exact differentiation (SOED) [46], [47] is employed as follows:

$$\begin{aligned} \dot{\chi}_0 &= w_0 \\ w_0 &= -a_1 |\chi_0 - x_1|^{2/3} \, sign\,(\chi_0 - x_1) + \chi_1 \\ \dot{\chi}_1 &= w_1 \\ w_1 &= -a_2 |\chi_1 - w_0|^{2/3} \, sign\,(\chi_1 - w_0) + \chi_2 \\ \dot{\chi}_2 &= -a_3 sign\,(\chi_2 - w_1) \end{aligned} \quad (18)$$

where a_1, a_2, and a_3 are chosen as suitable positive parameters.

Then, the estimation of velocity and acceleration can be reached as

$$\chi_1 = \dot{y}, \ \chi_2 = \ddot{y}. \quad (19)$$

B. FAULT DETECTION AND IDENTIFICATION USING TIME DELAY ESTIMATION

After obtaining the new linear model, in order to effectively reduce the effect of disturbance/uncertainty as well as faults, the time delay estimation is proposed to estimate the new lumped disturbance. Then, robust FTC considering the FDTDE result can be investigated to compensate for the influence of the lumped disturbance and faults in the EHA system.

From (17), at time t, the new lumped disturbance is given by the following.

$$\Omega(t) = \dot{\psi}(t) - A\psi(t) - Bv(t) \quad (20)$$

Hence, the TDE technique is used to determine $\Omega(t)$ through $\Omega(t - t_d)$ that can be expressed as

$$\hat{\Omega} = \Omega(t - t_d) = \dot{\psi}(t - t_d) - A\psi(t - t_d) - Bv(t - t_d) \quad (21)$$

where t_d is the estimation time-delay. Mostly, t_d is the sampling time interval and $\hat{\Omega} = [0 \ 0 \ \hat{\delta}]^T$ is the estimated value of Ω.

The equation (21) indicates that the lumped disturbance can be formulated from the known dynamics of the linearized system and control input.

Following Appendix A, the new lumped uncertainty includes lumped disturbance $f_d(d_1, d_2)$ (i.e., matched disturbance and mismatched disturbance) and fault $\varphi_f(f_a)$. The estimated new lumped uncertainty can be re-expressed as

$$\hat{\Omega} = \hat{f}_d + \hat{\varphi}_f = f_d(t - t_d) + \varphi_f(t - t_d) \quad (22)$$

To realize the detection system fault process, a threshold μ is determined through conducting experiments under healthy and faulty conditions. In the case of the absence of the internal leakage fault, following (4), $\varphi_f(f_a) = 0$ when $t < T_m$. Then, according to (22), one obtains

$$\Omega = f_d(t) \leq \mu \quad (23)$$

Inspired by the FDTDE, relying on the predefined threshold value, the fault is detected immediately when $\hat{\Omega} > \mu$. In practice, to determine the threshold, the control system without fault is firstly tested to evaluate the limitations as well as the influence of the matched and mismatched terms $f_d(d_1, d_2)$. Then, the threshold is selected bigger than the upper bound of $f_d(d_1, d_2)$. It is concluded that the FD system guarantees sensitive to the leakage fault, however, it also suppresses the impact of lumped uncertainty of the system.

C. CONTROL LAW DESIGN

In this sub-section, the combining of the FBL, TDE, and AISMC is investigated to not only enhance the tracking control accuracy but also achieve system stability in the presence of disturbances/uncertainties and actuator faults. Input-output feedback linearization is developed to alleviate the nonlinearity of the system. Then, the ISMC is applied to reduce steady-state error and pursue the finite-time stability for the

EHA. The robustness of the controller is enhanced to against the appearance of fault and the TDE error with the assist of the adaption gain parameter. Moreover, the new lumped disturbance is approximated by the FDTDE technique. It is efficiently compensated through the proposed control algorithm and helpfully improves the tracking performance. The stability of the whole system is verified using the Lyapunov method.

The tracking errors of the linearized system are defined as

$$e_{\psi_i} = \psi_{id} - \psi_i, \ i = \overline{1, 3} \tag{24}$$

where $\psi_d = [\psi_{1d} \ \psi_{2d} \ \psi_{3d}]^T = [y_d \ \dot{y}_d \ \ddot{y}_d]^T$ is the desired trajectory.

The error dynamics are formulated as follows:

$$\begin{aligned} \dot{e}_{\psi_1} &= e_{\psi_2} \\ \dot{e}_{\psi_2} &= e_{\psi_3} \\ \dot{e}_{\psi_3} &= \dot{\psi}_{3d} - (v + \delta) \end{aligned} \tag{25}$$

The sliding mode control law is established to secure that the tracking error in (25) converges to zero. The sliding manifold is designed as

$$s = k_0 \int_0^t e_{\psi_1} d\tau + k_1 e_{\psi_1} + k_2 e_{\psi_2} + e_{\psi_3} \tag{26}$$

where k_0, k_1, and k_2 are positive constant; the integral component is supplemented to degrade the steady-state error, and these control gains are selected, in such a way, that the ideal conditions $s = 0$, and $\dot{s} = 0$ are satisfied.

To receive a good dynamic process, the gain parameters can be figured out by following the pole placement method.

$$p_s = (p + \varpi)^3 = p^3 + 3\varpi p^2 + 3\varpi^2 p + \varpi^3 \tag{27}$$

where p is Laplace operator, ϖ is a positive constant.

Hence, the poles are p_1, p_2, p_3 that lie in the left-half plane. So, (27) is a Hurwitz polynomial. The gain parameters are computed as follows:

$$k_0 = \varpi^3, k_1 = 3\varpi^2, k_2 = 3\varpi \tag{28}$$

The derivative of s can be represented as

$$\begin{aligned} \dot{s} &= k_0 e_{\psi_1} + k_1 \dot{e}_{\psi_1} + k_2 \dot{e}_{\psi_2} + k_3 \dot{e}_{\psi_3} \\ &= k_0 e_{\psi_1} + k_1 e_{\psi_2} + k_2 e_{\psi_3} + \dot{\psi}_{3d} - (v + \delta) \end{aligned} \tag{29}$$

To stabilize the system (17), with the estimated lumped uncertainty and fault in (22), the auxiliary control law is designed as follows:

$$v^* = \underbrace{v_{com} + v_{rob} + v_z}_{v_0} + v_{tde} \tag{30}$$

where v_{com} is a dynamics compensation term, v_{rob} is a robust term that is used to alleviate the estimation error, v_z helps the sliding surface from an arbitrary place back to the vicinity of zero, and v_{tde} is a lumped compensation term that is obtained by using TDE. These designs are given as follows:

$$\begin{aligned} v_{com} &= \dot{\psi}_{3d} + k_0 e_{\psi_1} + k_1 e_{\psi_2} + k_2 e_{\psi_3}; \\ v_{tde} &= -\hat{\delta}; \ v_z = k_s s; \ v_{rob} = \eta sign(s). \end{aligned} \tag{31}$$

where k_s, η are positive constants, and $\dot{\psi}_{3d} = y_d$.

Denotes $\tilde{\delta} = \delta - \hat{\delta}$ that is the estimation error of the lumped disturbance term.

Assumption 2: The boundedness of the time-delay estimation error $\tilde{\delta}$ is defined by D. This hypothesis has been verified in [13], [48] with a sufficiently small time delay t_d.

The robust gain η is investigated to cope with the occurrence of fault and the TDE error. To promote the robustness feature of the controller, the adaptive gain algorithm is developed. Hence, the robust component can be modified by

$$v_{rob} = \hat{\eta} sign(s) \tag{32}$$

where $\hat{\eta}$ is the adapt value of the gain η

The effective gain adaption is given by

$$\dot{\hat{\eta}} = \Gamma^{-1} |s| \tag{33}$$

where Γ is a positive adaption parameter.

According to Appendix A, $L_\varphi L_\phi^2 \xi \neq 0$, the relative degree equals 3 and the feedback control law is constructed as follows:

$$u = \frac{1}{L_\varphi L_\phi^2 \xi} \left(v^* - L_\phi^3 \xi \right) \tag{34}$$

Theorem 1: Considering the system (6) satisfying Assumption 1, with the TDE in (21), if the control input signal is proposed as (34) together with the auxiliary control law (30), the adaptive law (33) that does not only guarantee the stability of the whole system but also retain acceptable tracking control in the event of faulty conditions, matched and mismatched disturbance.

Proof:

Let consider the candidate Lyapunov function

$$V = \frac{1}{2}s^2 + \frac{1}{2}\Gamma \left(\hat{\eta} - D\right)^2 \tag{35}$$

Taking the time derivative of V with noting (31), (33), one obtains

$$\begin{aligned} \dot{V} &= s\dot{s} + \Gamma \left(\hat{\eta} - D\right) \dot{\hat{\eta}} \\ &= s \left(k_0 e_{\psi_1} + k_1 e_{\psi_2} + k_2 e_{\psi_3} + \dot{\psi}_{3d} - (v + \delta)\right) \\ &\quad + \Gamma \left(\hat{\eta} - D\right) \dot{\hat{\eta}} \\ &= s \left(-k_s s - \hat{\eta} sign(s) - \tilde{\delta}\right) + \Gamma \left(\hat{\eta} - D\right) \dot{\hat{\eta}} \\ &= -k_s s^2 - \left(\hat{\eta} - D\right) \left(|s| - \Gamma \dot{\hat{\eta}}\right) - |s| \left(\tilde{\delta} sign(s) + D\right) \\ &\leq -k_s s^2 \end{aligned} \tag{36}$$

Then, the derivative of Lyapunov function $\dot{V}$ is negative semidefinite which shows that s will converge to zero in a certain time, and $e_{\psi_i} \to 0$ as $t \to \infty$. Thus, it can be concluded that the stabilization of the closed-loop system can be achieved according to Lyapunov criteria [49]. Theorem 1 is proved.

Remark 6: To eliminate the chattering phenomenon, the saturation function $sat(\cdot)$ is utilized to replace the $sign(\cdot)$

function in (32) as [13]

$$sat\left(\frac{s}{\varepsilon}\right) = \begin{cases} sign\,(s) & \text{if } |s| \geq \varepsilon \\ \frac{s}{\varepsilon} & \text{otherwise} \end{cases} \tag{37}$$

where ε is a small and positive coefficient.

Remark 7: To avoid the continuous increase of the adaptive gain in (33), some tips, e.g., dead-zone technique is developed to ensure the feasibility in practice as follows [50]:

$$\dot{\hat{\eta}} = \begin{cases} \Gamma^{-1}\,|s| & \text{if } |s| > \varepsilon_d \\ 0 & \text{otherwise} \end{cases} \tag{38}$$

where ε_d is a small positive scalar.

Remark 8: From the developed control law, the guidelines to select the parameters are given as follows:

1) For fault detection, the threshold μ is carefully selected which is the boundness of the matched and mismatched terms $f_d(d_1, d_2)$.

2) For control module, a pole placement technique is used to select the desired pole ϖ. Next, the gain parameters k_0, k_1, k_2 of the sliding manifold are determined via (28). Then, the gain k_s is tuned to approach the switching manifolds faster. Lastly, the parameter adaption rate Γ is increased gradually to guarantee the convergence of the adaptive parameter. In addition, the effects on the system behavior will be evaluated by trial and error through simulation analysis and experimental tests.

IV. SIMULATION RESULTS
A. SIMULATION SETUP
In this part, the effectiveness of the proposed controller is demonstrated through numerical simulation and experiments using MATLAB Simulink software. The sampling time is set as $0.005s$ and the simulation time is chosen as $T = 30s$. The parameters of the EHA system via the identification process and the assumed parameters of matched, mismatched disturbance are provided in Table 1. For the purpose of comparison, the desired input signal is selected as $q_d = 20\sin(0.2\pi t - \pi/2)(mm)$.

To evaluate the improved performance of the suggested FTC, i.e., adaptive integral sliding mode feedback linearization controller using FDTDE, a PID controller, and a backstepping controller with TDE (BCTDE), in turn, have been derived for the EHA as a comparison. The design of relevant controllers is presented in Appendix B. The following control gain of the controllers are tuned via the trial error method or based on the trade-off between the convergence speed and oscillatory and shown as: BCTDE $k_{b1} = 15, k_{b2} = 100, k_{b3} = 20$; proposed controller $\varpi = 40$, $k_s = 5.5$, $\Gamma = 80$. The selection of threshold value is set as $\mu = 150$ in simulation. In the different control scheme, PID controller is tuned by Ziegler-Nichols method with $K_p = 120$, $K_i = 20$, $K_d = 0.001$.

For the sake measurement of the quality of each control algorithm, the root mean square (RMS) error (index 1) or

TABLE 1. Parameters of EHA system.

Symbol	Value	Symbol	Value
g_a	$1.5 \times 10^{-7}\,\text{m}^2/\text{kg}$	k_t	$3.2 \times 10^{-8}\,\text{m}^3/\text{s/V/Pa}^{-1/2}$
g_b	$100\,\text{N·s/(kg·m)}$	f_c	$10\,\text{N/kg}$
h_a	$1.6 \times 10^5\,\text{N}^{1/2}(\text{s·m}^3)$	F_{ext}	$2.5\,\text{N/kg}$
h_b	$50\,(1/\text{s})$	k_f	$10\,\text{N·s/(kg·m)}$
h_c	$2 \times 10^7\,\text{N/m}^2$	Q_{Li}	$1.4 \times 10^{-10}\,\text{m}^5/\text{Ns}$
P_s	$16\,\text{MPa}$	α	8

control effort (index 2) is computed as follows:

$$RMS = \sqrt{\frac{1}{N}\sum_{i=1}^{n} z_i^2} \tag{39}$$

where i and n are the current and total of sample number, respectively; z_i is the interested index for the current sample. The index 1 (*mm*) shows the tracking accuracy whilst the index 2 (*V*) evaluates the control effort.

In order to show the superior properties of the proposed control in case of the appearance of fault, two working scenarios are considered as

1. Both matched and mismatched disturbances, and without fault.

2. Simultaneous abrupt internal leakage fault, matched and mismatched disturbances.

B. SIMULATION RESULT
The effectiveness of the FDTDE is firstly validated for detection and identification of the internal leakage fault in the simulation. As the above-mentioned analysis, the matched, mismatched, and fault is integrated into the new lumped uncertainty through the coordinate transformation. Then, the FDTDE is applied to exactly estimate it. The estimation results in the absence of fault are displayed in Fig. 3a. From Fig. 3a, we can see that the FDTDE brings a high accuracy estimation. And the selection threshold preserves the boundness of the new lumped uncertainty under healthy conditions. A fault is subsequently generated with internal leakage coefficient $C_{t0} = 2.5 \times 10^{-8} m^4/(N^{1/2}s)$. When the fault happens at the time $t = 6s$, the estimated lumped uncertainty overshoots the predetermined threshold. The response of the residual in the occurrence of the fault is depicted in Fig. 3b. From this figure, in the presence of the fault, it is clear that the fault has been successfully detected and accurately estimated thanks to the FDTDE.

1) SCENARIO 1
In this working scenario, the system operates in healthy condition, the fault does not occur. Meanwhile, there exists the matched and mismatched disturbance, the FDTDE is used to approximate the uncertainty component. We investigate the performance comparison of the proposed FTC with the PID and BCTDE. The comparisons of three controllers including
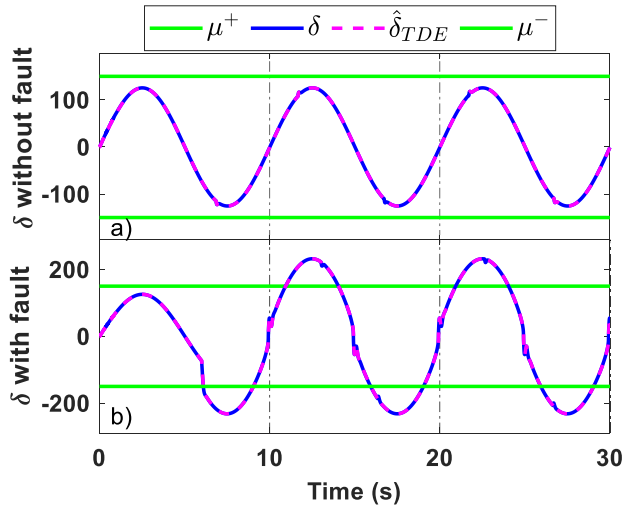
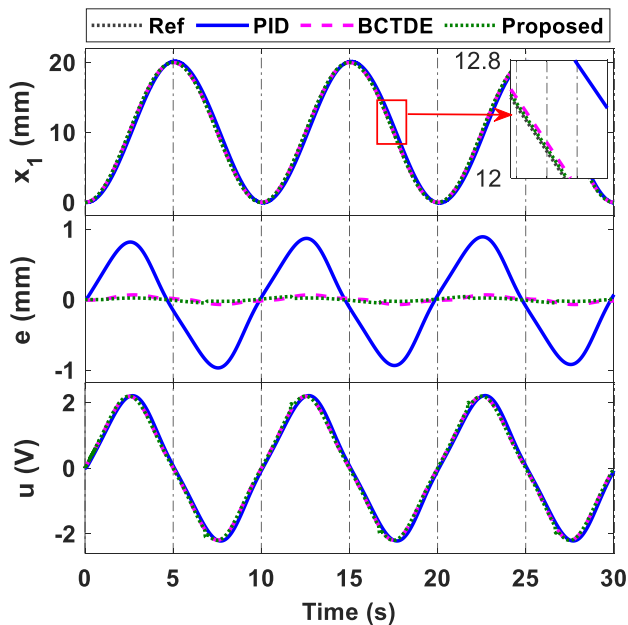**FIGURE 3.** Lumped disturbance estimation in simulation: a) without fault, b) abrupt fault.

FIGURE 4. Performances of three controllers in simulation, scenario 1.

FIGURE 5. Performances of three controllers in simulation, scenario 2.

TABLE 2. Performance indices of three controllers in simulation.

	Controller	PID	BCTDE	Proposed
Scenario 1	Index 1	0.6031	0.0410	0.0229
	Index 2	1.4671	1.4464	1.3527
Scenario 2	Index 1	0.8301	0.3812	0.1824
	Index 2	2.0179	1.9940	1.9776

the tracking position, the error state, and the control input are shown in Fig. 4. As can be seen in Fig. 4, due to the assist of the TDE, the lumped uncertainty is compensated. Except for PID, the relevant methods have no significant differences, the response is still ensured with small errors. It is observed that the performance of the PID controller was worse in presence of the lumped uncertainty due to the lack of uncertainty compensation. The BCTDE has a larger tracking error than the proposed controller because of non-possession a robustness term to tackle the certain estimation error of the TDE. Furthermore, from the performance indices in Table 2, the PID, BCTDE, and proposed controllers lead to the RMS errors of 0.6031, 0.041, and 0.0229 mm, respectively. Whilst the three controllers consume the RMS
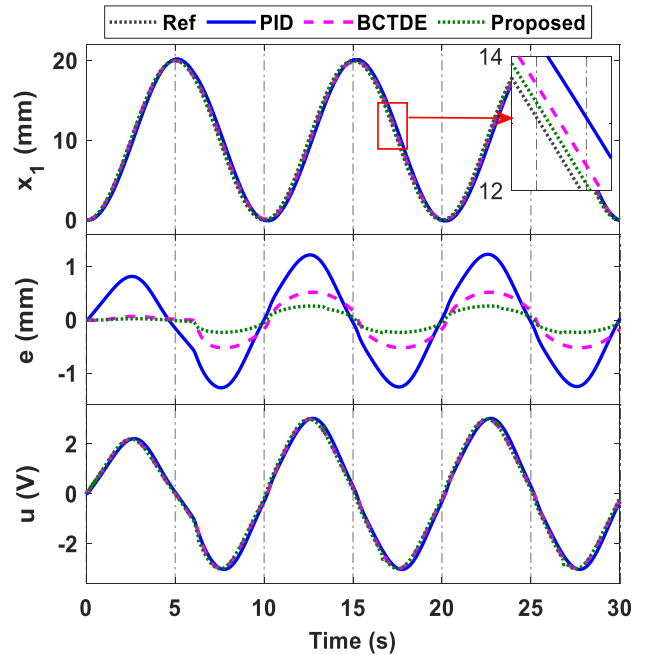
control efforts of 1.4671, 1.4464, and 1.3527 V, respectively. Evidently, the suggested controller complementing the adaptive gain and integral term yields the best performance with minimum tracking error and the requirement of the lowest control effort.

2) SCENARIO 2

In order to verify the robustness of the proposed controller, the abrupt internal leakage fault is augmented as a partial loss of effectiveness. It is noteworthy that the fault changes from slight to abrupt depending on the evolution rate and the internal leakage coefficient [37], however, the abrupt fault is only presented in this article. So, the internal leakage coefficient is chosen as $C_{t0} = 2.5 \times 10^{-8} m^4/(N^{1/2}s)$ to indicate the influence of the internal leakage fault and the time of the occurrence fault is $6s$. The transient responses of the output position, the error state, and the control input, in turn, are illustrated in Fig. 5. It can be seen that the control effort of relevant controllers is significantly changed to against both disturbance and the fault at the time $6s$. On the other hand, the comprise of adaptive gain and TDE upgrades the effectiveness of the suggested methodology which is visibly evident from the error state plot. Hence, we can see that the proposed FTC provided better performance than the BCTDE
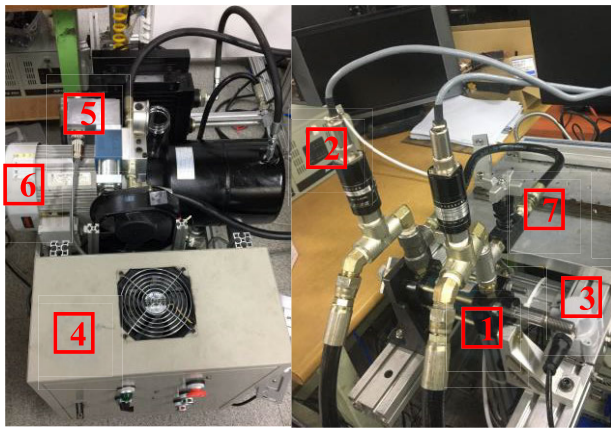
FIGURE 6. The experimental bench of EHS (1–a double rod cylinder, 2–pressure sensor, 3–wire sensor, 4–control box, 5–servo valve, 6–hydraulic power, 7–valve flow to generate leakage fault).

FIGURE 7. Lumped disturbance estimation in experiment: a) without fault, b) abrupt fault.

FIGURE 8. Performances of three controllers in experiment, scenario 1.

and PID despite the addition of internal leakage fault. The RMS error and the effort of signal control of three controllers in the simulation are shown in Table 2 that again confirmed the effectiveness of the proposed FTC.
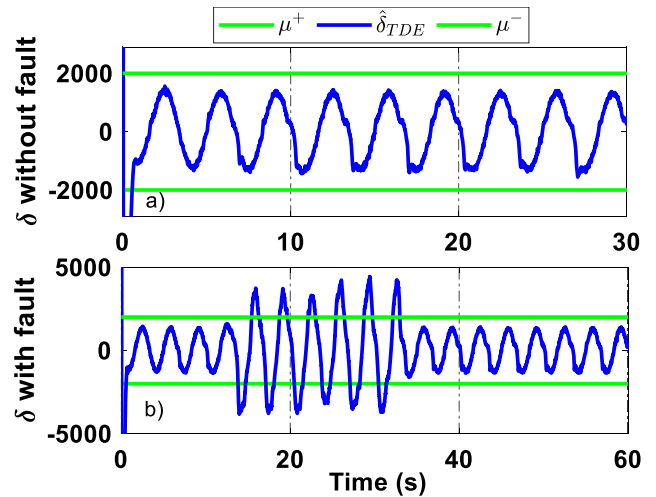
V. EXPERIMENTAL VERIFICATION

The experiment setup is depicted in Fig. 6. The EHA system includes a double-rod cylinder which is controlled by a servo valve, a hydraulic power unit, measurement system (two pressure sensors and displacement transducer). Besides, a NI PCI-6014 with a computer system was set up. The setting parameters for the real EHA system are shown in Table 3.
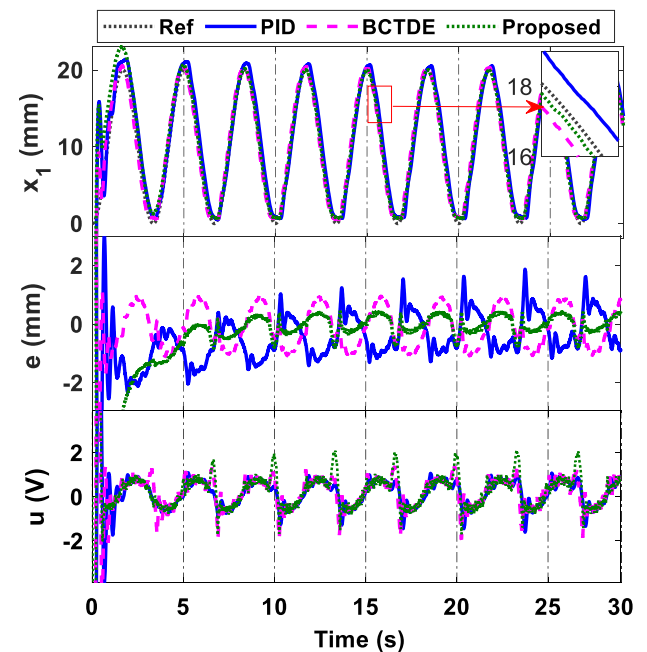
TABLE 3. Setting parameters of the real EHA system.

Components	Parameters	Specification
Double-rod cylinder	Tube diameter	36 [mm]
	Rod diameter	12 [mm]
	Length of stroke	25 [mm]
Servo valve	Model	MOOG – D633-317B
	Rated flow	10 [l/min]
Pressure sensor	Capacity	300 [bar]
	Rated output	30 [bar/V]
Displacement transducer	Model	Rational WTB5-0500MM
	Resolution	0.005mm
DAQ Card	Model	PCI-6014
	Resolution	AI/AO: 16 bit
Hydraulic Pump	Displacement	3.6 [cc/rev]
	Rated rotation speed	1730 [rpm]
	Relief pressure	160 [bar]

The artificial internal leakage fault is generated through a manual flow control valve that connects two chambers of the hydraulic cylinder. The threat level of the fault depends on the range adjustment of the flow control valve. Considering the mechanical limitation of the length of the cylinder stroke, the reference trajectory is chosen as $q_d = 20sin(0.6\pi t - \pi/2)(mm)$. In the experiment, all the parameters of the EHA system, as well as the control gains, are set similar to the corresponding values in simulation.

The sequent implementing experimental is the same as in simulation. The experiment results are shown in Figs. 7 – 11. First of all, the effectiveness of the FDTDE is confirmed and the threshold value is again determined for suitable in practice, $\mu = 2 \times 10^3$ in Fig. 7a. When the flow control valve is adjusted to create the internal leakage fault at the time $t = 12s$, the lumped estimation including matched, mismatched disturbance, and fault, is larger than the threshold. The fault is successfully detected in Fig. 7b. Next, two experiment scenarios are exploited corresponding to with and without the appearance of fault.

A. SCENARIO 1
This working scenario considers the situation that there are matched and mismatched disturbance from the EHA system
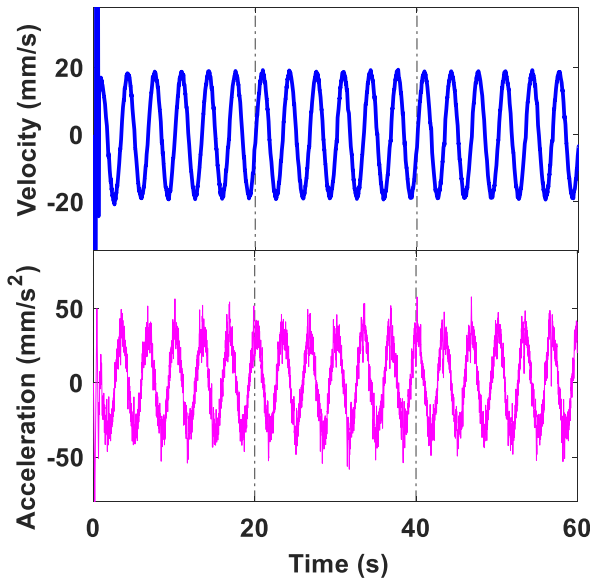
FIGURE 9. Estimated velocity and acceleration of SEOD in experiment.

TABLE 4. Performance indices of three controllers in experiment.

	Controller	PID	BC-TDE	Proposed
Scenario 1	Index 1	0.7118	0.6794	0.3062
	Index 2	0.7238	0.7004	0.6955
Scenario 2	Index 1	1.7910	0.9770	0.3597
	Index 2	1.7329	1.6639	1.6020

whilst a fault doesn't appear. The corresponding experimental results of scenario 1 are depicted in Figs. 8. It is obvious that the traditional PID controller presents large errors in presence of lumped uncertainties. Although the lumped uncertainties are compensated by the TDE, the BCTDE is still poorer than the suggested controller because of not belonging any measure to treat the undesired estimation error as well as the deviation in the parameter identification method for the EHA system. In contrast, the proposed controller provides a significant improvement of the performance due to the robustness properties of the adaptive law as well as the ISMC technique to alleviate the estimation error. The performance indices of the comparative controllers are calculated from $t = 10s$ and described in Table 4. It can be seen that the tracking accuracy of the proposed controller has been improved by 57% and 54% over PID and BCTDE methods, respectively. The result of data analysis proves the superior properties of the proposed control compared to the remaining controllers. Fig. 9 illustrates the velocity and acceleration estimation via the constructed SEOD. As shown, the information via the SOED can be given by differential and filtering, which facilitates for the control design procedure of the proposed controller.

B. SCENARIO 2
In the experiment of scenario 2, the robustness of the suggested method is validated under the matched, mismatched
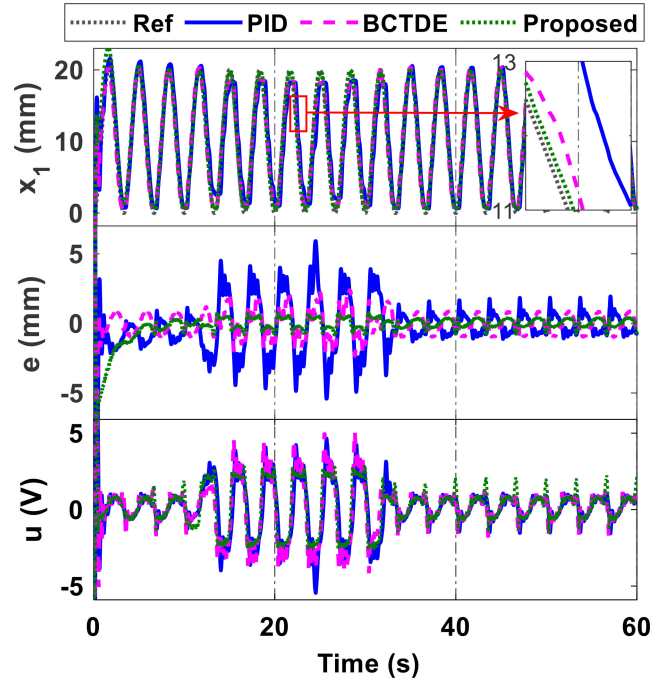

FIGURE 10. Performances of three controllers in experiment, scenario 2.
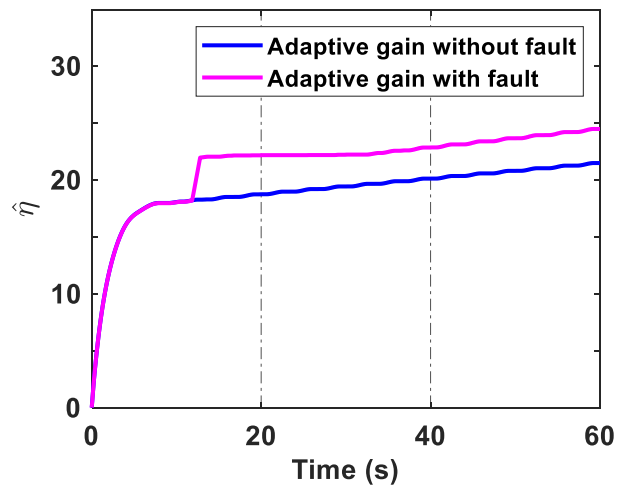

FIGURE 11. Adaptive gain in experiment.

and internal leakage fault. The abrupt fault is generated by the manual flow control valve. Because of the serious damage and safety problem in the appearance of the fault, the fault experiment is implemented from $12s$ to $33s$. The experiment results are shown in Fig. 10. As seen in this figure, the control performance of the PID and BCTDE became much worse in the heavy fault condition. The control effort and the error state significantly increase at the time $t = 12s$. These results are explained by the insufficient compensation of relevant controllers against the abrupt fault. Meanwhile, due to the robust FTC scheme, a great improvement was achieved by taking the advantage of the integration of TDE into the integral sliding mode, FBL technique, and adaptable property. The efficiency of comparative controllers is evaluated through RMS error

in Table 4. The RMS tracking errors of PID, BCTDE, suggested controller, in turn, are obtained as 1.791, 0.977 and 0.3597 *mm*. In addition, RMS control efforts are calculated as 1.7329, 1.6639, and 1.6020 *V*, respectively. It reveals that the outstanding efficiency of the proposed control algorithm once again is confirmed in case of the occurrence of faults.

Furthermore, the responses of the adaptive gains for two working scenarios are illustrated in Fig. 11. It can be observed from Fig. 11 that this parameter is adapted to suppress the effects on the appearance of fault and TDE error. Since the fault occurs at time $t = 12s$, the adaption gain, ie, $\hat{\eta}$ will be significantly regulated to approximate the value η, and then, to further enhance the tracking performance.

Therefore, the simulation and experiment results indicate that the suggested fault-tolerant controller can be applied for EHA and exhibits the best performance despite the matched, mismatched disturbances, and internal leakage fault.

VI. CONCLUSION

On the premise of the synthesis of adaptive integral sliding mode, feedback linearization technique, and time delay estimation, the proposed FTC scheme has been investigated in this article. Firstly, the descriptor of the EHA system in presence of matched, mismatched disturbance, and internal leakage fault is established. Then, we linearize the nonlinear EHA system by using the coordinate transformation. Next, the new lumped disturbance including disturbance/uncertainty, and the concerned fault is estimated by the assist of the TDE. Moreover, the TDE-based fault detection is developed. Lastly, the incorporation of adaptive integral sliding mode-based feedback linearization technology and TDE is proposed to guarantee the high precision tracking control and maintain the stability system in spite of disturbances as well as faults. The Lyapunov approach is used to verify the stability of the closed-loop system. The simulation analyses and experiment results have been demonstrated the efficiency of the suggested methodology. In future work, the development of the proposed FTC will be studied to deal with the simultaneous faults, i.e., sensor fault, actuator fault and achieve the asymptotic tracking performance.

APPENDIX A

In this appendix, the vector relative degree of the system (9) is computed through the differentiation of the output y until the condition $L_\varphi L_\phi^{\rho-1} \xi \neq 0$ is satisfied.

$$L_\varphi \xi = 0; \; L_d \xi = 0; \; L_\phi \xi = x_2; \; L_\varphi L_\phi \xi = 0;$$
$$L_d L_\phi \xi = -(k_f x_2 + f_c tanh(x_2) + F_{ext}); \; L_\phi^2$$
$$\xi = g_a x_3 - g_b x_2;$$
$$L_\varphi L_\phi^2 \xi = g_a h_a \sqrt{P_s - x_3 tanh(u)} \neq 0;$$
$$L_d L_\phi^2 \xi = g_a h_d (Q_{Li} - C_t \sqrt{|x_3|} tanh(x_3))$$
$$+ g_b (k_f x_2 + f_c tanh(x_2) + F_{ext})$$
$$= -g_b d_1 + g_a (d_2 + f_a);$$

$$\frac{d^2}{dt^2} (L_d \xi) = \frac{d}{dt} (L_d \xi) = 0;$$
$$L_\phi^3 \xi = -g_b (g_a x_3 - g_b x_2) - g_a (h_b x_3 + h_c x_2);$$
$$\frac{d}{dt} (L_d L_\phi \xi) = \dot{d}_1 = (f_c tanh(x_2)^2 - k_f - f_c)(g_a x_3 - g_b x_2)$$
$$+ (k_f + f_c - f_c tanh(x_2)^2)$$
$$\times (k_f x_2 + f_c tanh(x_2) + F_{ext});$$
$$\delta = L_d L_\phi^2 \xi + \frac{d}{dt} (L_d L_\phi \xi) + \frac{d^2}{dt^2} (L_d \xi)$$
$$= \underbrace{\dot{d}_1 - g_b d_1 + g_a d_2}_{f_d(d_1,d_2)} + \underbrace{g_a f_a}_{\varphi_f(f_a)}$$

Because $L_\varphi L_\phi^2 \xi \neq 0$, the relative degree ρ of (9) is 3, and equals to the system dimension. So, the whole nonlinear system dynamics are fully linearized.

APPENDIX B

This appendix presents the detailed design of comparative controllers.

1) The traditional PID controller law was designed as

$$u = K_p e_{\psi_1} + K_d \dot{e}_{\psi_1} + K_i \int_0^t e_{\psi_1}(t) \, dt \quad (40)$$

where K_p, K_d, and K_i are the proportional gain, the derivative gain, and the integral gain, respectively.

2) In [51], [52] A TDE-based control using backstepping technique (BCTDE) was proposed. The TDE is given as:

$$\hat{d} = d(t - t_d) = \dot{x}(t - t_d) - \phi(t - t_d) + \varphi(t - t_d) u \quad (41)$$

where $\hat{d} = \begin{bmatrix} 0 & \hat{d}_1 & \hat{d}_2 \end{bmatrix}^T$ is the estimation value of d.

The backstepping controller was presented as follows:

Denote $e_i = x_i - x_{id}; \; i = \overline{1,3}$ as the errors between the measurement values and the virtual signals. Herein, to achieve the desired tracking performance, the virtual and final control law of BC can be designed as

$$x_{2d} = \dot{x}_{1d} - k_{b1} e_1; \; \dot{e}_1 = x_2 - \dot{x}_{1d}; \; \dot{x}_{2d} = \ddot{x}_{1d} - k_{b1} \dot{e}_1;$$
$$x_{3d} = \frac{1}{g_a} \left(\dot{x}_{2d} - g_b x_2 - \hat{d}_1 - k_{b2} e_2 - e_1 \right);$$
$$u = \frac{1}{h_a \sqrt{P_s - x_3 sign(u)}}$$
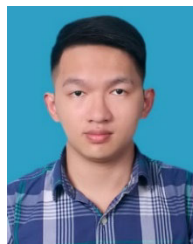$$\times (\dot{x}_{3d} + h_b x_2 - \hat{d}_2 - k_{b3} e_3 - e_2); \quad (42)$$

where k_{b1}, k_{b2}, and k_{b3} are positive gain parameters.

REFERENCES

[1] Z. Yao, J. Yao, and W. Sun, "Adaptive RISE control of hydraulic systems with multilayer neural-networks," *IEEE Trans. Ind. Electron.*, vol. 66, no. 11, pp. 8638–8647, Nov. 2019.

[2] Q. N. Xu, K. M. Lee, H. Zhou, and H. Y. Yang, "Model-based fault detection and isolation scheme for a rudder servo system," *IEEE Trans. Ind. Electron.*, vol. 62, no. 4, pp. 2384–2396, Apr. 2015.

[3] V. D. Phan, C. P. Vo, H. V. Dao, and K. K. Ahn, "Robust fault-tolerant control of an electro-hydraulic actuator with a novel nonlinear unknown input observer," *IEEE Access*, vol. 9, pp. 30750–30760, 2021.

[4] J. Yao, "Model-based nonlinear control of hydraulic servo systems: Challenges, developments and perspectives," *Frontiers Mech. Eng.*, vol. 13, no. 2, pp. 179–210, Jun. 2018.

[5] X. Liu, H. Yu, J. Yu, and L. Zhao, "Combined speed and current terminal sliding mode control with nonlinear disturbance observer for PMSM drive," *IEEE Access*, vol. 6, pp. 29594–29601, 2018.

[6] S. D. Lee and S. Jung, "A Monte Carlo dual-RLS scheme for improving torque sensing without a sensor of a disturbance observer for a CMG," *Int. J. Control, Autom. Syst.*, vol. 18, no. 6, pp. 1530–1538, Jun. 2020.

[7] J. Liu, W. Gai, J. Zhang, and Y. Li, "Nonlinear adaptive backstepping with ESO for the quadrotor trajectory tracking control in the multiple disturbances," *Int. J. Control, Autom. Syst.*, vol. 17, no. 11, pp. 2754–2768, Nov. 2019.

[8] W. Deng, J. Yao, Y. Wang, X. Yang, and J. Chen, "Output feedback backstepping control of hydraulic actuators with valve dynamics compensation," *Mech. Syst. Signal Process.*, vol. 158, Sep. 2021, Art. no. 107769.

[9] X. Shao, L. Xu, and W. Zhang, "Quantized control capable of appointed-time performances for quadrotor attitude tracking: Experimental validation," *IEEE Trans. Ind. Electron.*, early access, May 18, 2021, doi: 10.1109/TIE.2021.3079887.

[10] G. Yang, J. Yao, and N. Ullah, "Neuroadaptive control of saturated nonlinear systems with disturbance compensation," *ISA Trans.*, Apr. 2021, doi: 10.1016/j.isatra.2021.04.017.

[11] X. Shao and Y. Shi, "Neural-network-based constrained output-feedback control for MEMS gyroscopes considering scarce transmission bandwidth," *IEEE Trans. Cybern.*, early access, May 25, 2021, doi: 10.1109/TCYB.2021.3070137.

[12] X. Shao, Y. Shi, W. Zhang, and H. Cao, "Neurodynamic approximation-based quantized control with improved transient performances for micro-electromechanical system gyroscopes: Theory and experimental results," *IEEE Trans. Ind. Electron.*, vol. 68, no. 10, pp. 9972–9983, Oct. 2021.

[13] C. P. Vo, X. D. To, and K. K. Ahn, "A novel adaptive gain integral terminal sliding mode control scheme of a pneumatic artificial muscle system with time-delay estimation," *IEEE Access*, vol. 7, pp. 141133–141143, 2019.

[14] C. Xia, G. Jiang, W. Chen, and T. Shi, "Switching-gain adaptation current control for brushless DC motors," *IEEE Trans. Ind. Electron.*, vol. 63, no. 4, pp. 2044–2052, Apr. 2015.

[15] W. Shen and J. Wang, "Adaptive fuzzy sliding mode control based on Pi-sigma fuzzy neutral network for hydraulic hybrid control system using new hydraulic transformer," *Int. J. Control, Autom. Syst.*, vol. 17, no. 7, pp. 1708–1716, Jul. 2019.

[16] W. Deng and J. Yao, "Extended-state-observer-based adaptive control of electrohydraulic servomechanisms without velocity measurement," *IEEE/ASME Trans. Mechatronics*, vol. 25, no. 3, pp. 1151–1161, Jun. 2020.

[17] X. Shao, Z. Cao, and H. Si, "Neurodynamic formation maneuvering control with modified prescribed performances for networked uncertain quadrotors," *IEEE Syst. J.*, early access, Oct. 22, 2020, doi: 10.1109/JSYST.2020.3022901.

[18] A. Shiralkar, S. Kurode, R. Gore, and B. Tamhane, "Robust output feedback control of electro-hydraulic system," *Int. J. Dyn. Control*, vol. 7, no. 1, pp. 295–307, Mar. 2019.

[19] Z. Gao, C. Cecati, and S. X. Ding, "A survey of fault diagnosis and fault-tolerant techniques—Part I: Fault diagnosis with model-based and signal-based approaches," *IEEE Trans. Ind. Electron.*, vol. 62, no. 6, pp. 3757–3767, Jun. 2015.

[20] X. Zhu and D. Li, "Robust fault estimation for a 3-DOF helicopter considering actuator saturation," *Mech. Syst. Signal Process.*, vol. 155, Jun. 2021, Art. no. 107624.

[21] T. Li, T. Yang, Y. Cao, R. Xie, and X. Wang, "Disturbance-estimation based adaptive backstepping fault-tolerant synchronization control for a dual redundant hydraulic actuation system with internal leakage faults," *IEEE Access*, vol. 7, pp. 73106–73119, 2019.

[22] H. V. Dao, D. T. Tran, and K. K. Ahn, "Active fault tolerant control system design for hydraulic manipulator with internal leakage faults based on disturbance observer and online adaptive identification," *IEEE Access*, vol. 9, pp. 23850–23862, 2021.

[23] S. Sharifi, A. Tivay, S. M. Rezaei, M. Zareinejad, and B. Mollaei-Dariani, "Leakage fault detection in electro-hydraulic servo systems using a nonlinear representation learning approach," *ISA Trans.*, vol. 73, pp. 154–164, Feb. 2018.

[24] J. Kim, H. Choi, and J. Kim, "A robust motion control with antiwindup scheme for electromagnetic actuated microrobot using time-delay estimation," *IEEE/ASME Trans. Mechatronics*, vol. 24, no. 3, pp. 1096–1105, Jun. 2019.

[25] D. Li, L. Wei, T. Song, and Q. Jin, "Study on asymptotic stability of fractional singular systems with time delay," *Int. J. Control, Autom. Syst.*, vol. 18, no. 4, pp. 1002–1011, Apr. 2020.

[26] F. Guo and P. Lu, "Improved adaptive integral-sliding-mode fault-tolerant control for hypersonic vehicle with actuator fault," *IEEE Access*, vol. 9, pp. 46143–46151, 2021.

[27] Y.-J. Liu, Q. Zeng, S. Tong, C. L. P. Chen, and L. Liu, "Actuator failure compensation-based adaptive control of active suspension systems with prescribed performance," *IEEE Trans. Ind. Electron.*, vol. 67, no. 8, pp. 7044–7053, Aug. 2020.

[28] Y. Li, K. Sun, and S. Tong, "Observer-based adaptive fuzzy fault-tolerant optimal control for SISO nonlinear systems," *IEEE Trans. Cybern.*, vol. 49, no. 2, pp. 649–661, Feb. 2019.

[29] M. Van and S. S. Ge, "Adaptive fuzzy integral sliding-mode control for robust fault-tolerant control of robot manipulators with disturbance observer," *IEEE Trans. Fuzzy Syst.*, vol. 29, no. 5, pp. 1284–1296, May 2021.

[30] J. Qin, Q. Ma, H. Gao, and W. X. Zheng, "Fault-tolerant cooperative tracking control via integral sliding mode control technique," *IEEE/ASME Trans. Mechatronics*, vol. 23, no. 1, pp. 342–351, Feb. 2018.

[31] C. P. Vo, V. D. Phan, T. H. Nguyen, and K. K. Ahn, "A compact adjustable stiffness rotary actuator based on linear springs: Working principle, design, and experimental verification," *Actuators*, vol. 9, no. 4, p. 141, Dec. 2020.

[32] H. A. Mintsa, R. Venugopal, J.-P. Kenne, and C. Belleau, "Feedback linearization-based position control of an electrohydraulic servo system with supply pressure uncertainty," *IEEE Trans. Control Syst. Technol.*, vol. 20, no. 4, pp. 1092–1099, Jul. 2012.

[33] C. Liu, G. Liu, and J. Fang, "Feedback linearization and extended state observer-based control for rotor-AMBs system with mismatched uncertainties," *IEEE Trans. Ind. Electron.*, vol. 64, no. 2, pp. 1313–1322, Feb. 2017.

[34] G. Yang and J. Yao, "Output feedback control of electro-hydraulic servo actuators with matched and mismatched disturbances rejection," *J. Franklin Inst.*, vol. 356, no. 16, pp. 9152–9179, Nov. 2019.

[35] J. Guo, "Robust tracking control of variable stiffness joint based on feedback linearization and disturbance observer with estimation error compensation," *IEEE Access*, vol. 8, pp. 173732–173754, 2020.

[36] G. Yang, J. Yao, G. Le, and D. Ma, "Adaptive integral robust control of hydraulic systems with asymptotic tracking," *Mechatronics*, vol. 40, pp. 78–86, Oct. 2016.

[37] J. Yao, G. Yang, and D. Ma, "Internal leakage fault detection and tolerant control of single-rod hydraulic actuators," *Math. Problems Eng.*, vol. 2014, pp. 1–14, Mar. 2014.

[38] D. T. Tran, D. X. Ba, and K. K. Ahn, "Adaptive backstepping sliding mode control for equilibrium position tracking of an electrohydraulic elastic manipulator," *IEEE Trans. Ind. Electron.*, vol. 67, no. 5, pp. 3860–3869, May 2020.

[39] G. Yang, H. Wang, and J. Chen, "Disturbance compensation based asymptotic tracking control for nonlinear systems with mismatched modeling uncertainties," *Int. J. Robust Nonlinear Control*, vol. 31, no. 8, pp. 2993–3010, May 2021.

[40] Q. Guo and Z. Chen, "Neural adaptive control of single-rod electrohydraulic system with lumped uncertainty," *Mech. Syst. Signal Process.*, vol. 146, Jan. 2021, Art. no. 106869.

[41] H.-Z. Tan and N. Sepehri, "Parametric fault diagnosis for electrohydraulic cylinder drive units," *IEEE Trans. Ind. Electron.*, vol. 49, no. 1, pp. 96–106, Aug. 2002.

[42] C. Kaddissi, J. P. Kenne, and M. Saad, "Identification and real-time control of an electrohydraulic servo system based on nonlinear backstepping," *IEEE/ASME Trans. Mechatronics*, vol. 12, no. 1, pp. 12–22, Feb. 2007.

[43] G. A. Sohl and J. E. Bobrow, "Experiments and simulations on the nonlinear control of a hydraulic servosystem," *IEEE Trans. Control Syst. Technol.*, vol. 7, no. 2, pp. 238–247, Mar. 1999.

[44] M. B. Souza, L. D. M. Honório, and E. J. Oliveira, "Innovative analysis for parameter estimation quality," *Int. J. Control, Automat. Syst.*, vol. 19, no. 1, pp. 363–371, Sep. 2020.

[45] A. A. Kabanov, "Feedback linearization of nonlinear singularly perturbed systems with state-dependent coefficients," *Int. J. Control, Autom. Syst.*, vol. 18, no. 7, pp. 1743–1750, Jul. 2020.

[46] A. Levant, "Robust exact differentiation via sliding mode technique," *Automatica*, vol. 34, no. 3, pp. 379–384, Mar. 1998.

[47] M. Van, S. S. Ge, and H. Ren, "Finite time fault tolerant control for robot manipulators using time delay estimation and continuous nonsingular fast terminal sliding mode control," *IEEE Trans. Cybern.*, vol. 47, no. 7, pp. 1681–1693, Jul. 2017.

[48] J. Lee, P. H. Chang, B. Yu, K.-H. Seo, and M. Jin, "An effective adaptive gain dynamics for time-delay control of robot manipulators," *IEEE Access*, vol. 8, pp. 192229–192238, 2020.

[49] H. K. Khalil, *Nonlinear Systems*. Upper Saddle River, NJ, USA: Prentice-Hall, 2002.

[50] M. Van, M. Mavrovouniotis, and S. S. Ge, "An adaptive backstepping nonsingular fast terminal sliding mode control for robust fault tolerant control of robot manipulators," *IEEE Trans. Syst., Man, Cybern., Syst.*, vol. 49, no. 7, pp. 1448–1458, Jul. 2018.

[51] J. Y. Lee, M. Jin, and P. H. Chang, "Variable PID gain tuning method using backstepping control with time-delay estimation and nonlinear damping," *IEEE Trans. Ind. Electron.*, vol. 61, no. 12, pp. 6975–6985, Dec. 2014.

[52] T. Jiang, F. Zhang, and D. Lin, "Finite-time backstepping for attitude tracking with disturbances and input constraints," *Int. J. Control, Autom. Syst.*, vol. 18, no. 6, pp. 1487–1497, Jun. 2020.

VAN DU PHAN received the B.S. degree in electrical engineering from Hanoi University of Science and Technology, Ha Noi, Vietnam, in 2013, and the M.Sc. degree in electrical engineering from Thai Nguyen University of Technology, Thai Nguyen, Vietnam, in 2017. He is currently pursuing the Ph.D. degree with the School of Mechanical Engineering, University of Ulsan, Ulsan, South Korea.

His research interests include soft robot, hydraulic robot, nonlinear control, and fault tolerant control.

CONG PHAT VO received the B.E. degree in electrical and electronic engineering technology and the M.Sc. degree in mechatronics engineering from Ho Chi Minh City University of Technology and Education, Vietnam, in 2013 and 2016, respectively, and the Ph.D. degree in mechanical and automotive engineering from the Department of Mechanical Engineering, University of Ulsan, Ulsan, South Korea, in 2021.

His research interests include intelligent control, soft robot, haptic control, and renewable energy.

HOANG VU DAO received the B.E. degree in mechatronics from the School of Mechanical Engineering, Hanoi University of Science and Technology, Vietnam, in 2018. He is currently pursuing the Ph.D. degree in mechanical engineering with the School of Mechanical Engineering, University of Ulsan, Ulsan, South Korea.

His current research interests include hydraulic robots, nonlinear control, and fault-tolerant control.

KYOUNG KWAN AHN (Senior Member, IEEE) received the B.S. degree from the Department of Mechanical Engineering, Seoul National University, in 1990, the M.Sc. degree in mechanical engineering from Korea Advanced Institute of Science and Technology (KAIST), in 1992, and the Ph.D. degree from Tokyo Institute of Technology, in 1999.

Since 2000, he has been with the School of Mechanical Engineering, University of Ulsan, where he is currently a Professor and the Director of the Fluid Power Control and Machine Intelligence Laboratory. His main research interests include fluid-based triboelectric nano generator, modeling and control of fluid power systems, energy saving construction machine, hydraulic robot, and power transmission in the ocean energy. He is the author or coauthor of over 190 SCI (E) papers and four books in these areas.

Prof. Ahn serves as an Editor for *International Journal of Control, Automation and Systems*. He serves on the Editorial Board for *Renewable Energy*, *Korean Fluid Power and Construction Machine*, and *Actuators*.

• • •